Mechanical Properties and Solubility Characteristics of PES-PCL Core-Shell Fibers Used as Nanofiber Substrates in Cell Migration Studies

Undergraduate Honors Research Thesis

Presented in Partial Fulfillment of the Requirements

for Graduation with Honors Research Distinction in Materials Science and Engineering

at The Ohio State University

By

Sravya Vajapeyajula

The Ohio State University

December, 2011

Project Advisor: Dr. John Lannutti, Professor, Materials Science and Engineering

Abstract

Culturing cells in 3D has been recognized as crucial for accurate data collection and interpretation. Electrospun nanofiber substrates are currently accepted by the scientific community as media that provide a 3D cell culture environment, or at least close to it. Previous and ongoing research in this area has mainly focused on characterizing nanofiber substrates composed of a single type of polymer such as PCL. Limited information exists on the mechanical and chemical properties of core-shell fibers that show great potential for application as drug delivery systems and tissue engineering scaffolds. This project was designed to expand available knowledge on core-shell fibers and their characteristics. To this end, electrospun PES-PCL core-shell fibers of varying core to shell volume ratios were tested in tension. The resulting data revealed that as the PCL (shell) content increases, the overall stiffness of the core-shell fibers also increases. In addition to tensile testing and SEM analysis, various solubility tests were conducted to identify a solvent that preferentially dissolves PCL over PES. This would help in future work to determine if the distinguishing properties of core-shell fibers are a result of the unique core-shell interactions or if they are simply the summation of individual core and shell properties. The following solvents were used in the solubility tests: Tetrahydrofuran (THF), chloroform, dichloromethane (DCM), and trichloroethylene (TCE). Of the solvents used, TCE showed the most selectivity for PCL. Pure PCL dissolved 100% in TCE while pure PES was mostly insoluble. However, PES-PCL core-shell fibers, though they exhibited greater solubility with increasing PCL content, did not exhibit weight loss proportional to % PCL content. SEM analysis revealed that exposing PES-PCL core-shell fibers to TCE results in webbing, which could have been the reason complete dissolution of PCL was not observed. This hypothesis was confirmed by solubility tests and subsequent SEM analysis of PCL/PES blends.

Table of Contents

List of Tables

List of Figures

Acknowledgments

I would like to thank Dr. John Lannutti for introducing me to the field of nanotechnology and giving me a chance to work in his lab. I am grateful for his guidance and help in not only this research project but also many other parts of my academic and professional life. I thank his patience, open-mindedness, and excellent mentorship that helped me in the successful completion of this project.

I would like to thank Dr. Jed Johnson for teaching me the basics of electrospinning and giving me timely tips and suggestions when I ran into electrospinning glitches. His knowledge and expertise helped me many times during the course of my research.

I would like to thank Dr. Nishant Tikekar for all his help with the SEM.

I would like to thank The Ohio State University College of Engineering for awarding me a scholarship to conduct research presented in this thesis.

Lastly, I would like to thank my parents and sisters for their encouragement and support throughout all of my endeavors.

1. Introduction

1.1 Background

Scientists for the last few decades have relied on cell culture to obtain preliminary data on new drugs or new procedures before they turned to animals for *in vivo* experiments. Even today, scientists use *in vitro* data to estimate what can be expected *in vivo.* Until recently, it was considered reasonable to assume that if cells interacted with a new substance in a certain way on the culture dish, living tissue composed of these same cells would interact similarly with that substance inside an organism. However, recent studies have shown that this assumption is wrong. It has been found that 2D glass or plastic platforms are very poor imitators of the 3D environment of live tissue and data obtained from 2D experiments provide inaccurate estimates of the cell response *in vivo*[1]. For instance, comparison studies examining cancer cell morphology have found that cancer cells cultured on 2D assume an unnatural, spread morphology while they adopt a clustered, rounded structure—which is more reminiscent of tumors *in vivo*—in 3D environments[2,3]. Furthermore, it has been shown that tumor cells cultured in 3D exhibit increased glycolysis[4] and different sensitivities to various anti-cancer drugs when compared to those cultured in 2D[5,6].

These differences have been observed in not just cancer cells. In fact, human skin cells cultured in 3D have been observed to be more resistant to oxidative stress and toxic heavy metals than the cells cultured in 2D. This led to the natural conclusion that dermatotoxicity testing is more likely to yield results comparable to true physiological responses if this testing is done on 3D culture substrates rather than 2D ones[7]. These results and many others led to the acceptance of 3D cell culture as the most viable method for obtaining accurate *in vitro* results.

There are several different 3D cell culture techniques available today. One of the widely accepted techniques involves using nanofiber substrates. Nanofiber substrates have been shown to be both biocompatible and good representations of live tissue. For instance, electrospun P(LLA-CL) was used recently to culture smooth muscle cells and endothelial cells. The results from this experiment showed that P(LLA-CL) is a good biomimetic extracellular matrix for cell culture because both the smooth muscle cells and endothelial cells adhered and proliferated well on these nanofiber scaffolds[8].

Synthetic hydrogels are another type of nanofiber scaffolds that allow cell culture in 3D. Modifying these synthetic, bioinert backgrounds with biologically active components has been shown to mimic the natural environment and yield results that are representative of *in vivo* response. For example, building an RGD peptide sequence that was susceptible to MMP-13 cleavage into a PEG gel upregulated chondrogenesis in the synthetic 3D environment as the removal of fibronectin does in vivo[9,10].

Another promising type of nanofiber scaffold that has potential for many biomedical applications, including use as 3D culture substrate, is the core-shell nanofiber. Core-shell fibers, as the name suggests, consist of a shell that is made of one substance and a core that is made of a different substance. Core-shell fibers show promise for an even closer imitation of native tissue than pure or blended nanofibers do. For instance, human dermal fibroblasts were cultured on PCL/Collagen core-shell fibers, collagen-coated PCL, and tissue culture plate. The results from this experiment showed that cell proliferation was greater on composite nanofibers, i.e. PCL-collagen core-shell fiber or collagen-coated PCL, than on pure nanofibrous PCL. Furthermore, cells were observed to penetrate beneath the PCL-collagen core-shell fibers while the same was not the case for the collagen-coated PCL or pure PCL[11]. This study shows the rising importance

of core-shell fibers in the quest for 3D cell culture environments. However, because core-shell electrospinning is a relatively new area of nanotechnology, limited information exists on the properties and mechanical characteristics of core-shell fibers. Thus, the research presented in this thesis was conducted to produce more information on core-shell fibers and their properties.

1.2 Project Objectives

This project had two main goals. The first was to determine the relationship between PES-PCL core-shell volume ratios and the overall stiffness of the resulting core-shell fiber. In other terms, the project was designed to answer the question: does the overall stiffness change with a change in proportion of PCL to PES and how does this change occur?

The second goal of the project was to identify a solvent that preferentially dissolves PCL, the shell. This could allow further investigation of core-shell properties and determine if the overall characteristics of the fiber are a summation of individual core and shell properties or if they are a result of unique core-shell interactions. It could also allow for investigation of the inherent properties of the nanofiber core once the shell is removed to help delineate how a shell can negatively influence—through fiber-fiber bonding—the composite properties.

2. Materials and Methods

2.1 Materials

2.1.1 Pure PCL

The pure PCL solution used in this experiment was 6.7 wt% polycaprolactone in 1,1,1,3,3,3-hexafluoro-2-propanol (HFP). This was prepared by transferring 3.35 g of PCL to a beaker situated on a mass balance and adding HFP to the beaker until the total mass of the solution was 50 g. The solution was then capped and sealed with parafilm. The sealed solution

was allowed to stir for 24 hours under a biosafety hood. The solution was then transferred to a 60 mL syringe equipped with a 20 gauge needle.

2.1.2 Pure PES

The pure PES solution used in this experiment was 8.0 wt% polyethersulfone in 1,1,1,3,3,3-hexafluoro-2-propanol (HFP). This was prepared by transferring 4.0 g of PES was added to the beaker and HFP was then added until the total mass of the solution was 50 g. The remaining steps are the same as those for the pure PCL solution.

2.1.3 PES/PCL Blends

The polymer blends used in this experiment were all 6.7 wt% solutions with HFP as the solvent. The three blends prepared were of the following solute compositions: (1) 5% PES, 95% PCL (2) 10% PES, 90% PCL, (3) 20% PES, 80% PCL. The first 5% PES blend was prepared by adding 0.10 g of PES to a beaker situated on a mass balance. 1.90 g of PCL was then transferred to this beaker and HFP added until the total mass of the solution was 30 g. The solution was then capped and sealed with parafilm. The polymer blend was stirred for 24 hours under a biosafety hood and transferred to a 60 mL syringe equipped with a 20 gauge needle.

The second 10% PES blend was prepared similarly. 0.20 g of PES was added to a beaker placed on a mass balance. 1.80 g of PCL was then transferred to the beaker and HFP was added until the total mass was 30 g. The rest of the steps were the same as those for the first blend.

The third 20% PES blend was prepared by transferring 0.40 g of PES and 1.60 g of PCL to a beaker and adding HFP until the total mass of the solution was 30 g. The rest of the steps were the same as those for the first blend.

2.2 Methods

2.2.1 Electrospinning

A metal plate wrapped in non-stick aluminum foil was placed on a platform. The ground wire of a high-voltage generator was attached to this plate. The syringe containing polymer solution was mounted on a syringe pump and this pump situated at a height such that the distance from the needle to the collection plate was 18 cm. The positive wire from the high-voltage was attached to the needle of the syringe. The syringe pump was set up so that the polymer solution was pumped at a continuous 13.0 mL/hr. Randomly oriented nanofibers were collected on the metal plate by applying +20 KV to the needle. The deposit time was 10 minutes.

2.2.2 Coaxial Spinning

A metal plate wrapped in non-stick aluminum foil was placed on a platform. The ground wire of a high-voltage generator was attached to this plate. The syringe containing the polymer solution for the core was mounted on a syringe pump situated at a height that allowed the distance from the needle to the collection plate to be 18 cm. The needle used in coaxial spinning is a concentric metallic needle. The syringe containing polymer solution for the shell was attached to a capillary tube and the other end of this capillary tube was attached to the concentric needle. This syringe was also mounted on an automatic syringe pump. The positive wire of the high-voltage generator was attached to the concentric needle. The feed rate of the core solution and the shell solution was adjusted according to the core-shell volume ratios desired. For instance, to achieve a 1:1 core-shell volume ratio, the feed rate of both the core and shell polymer solutions was 2 mL/hr. Randomly oriented core-shell fibers were collected by applying +20 KV to the needle. A schematic of this setup is given in Figure 1.

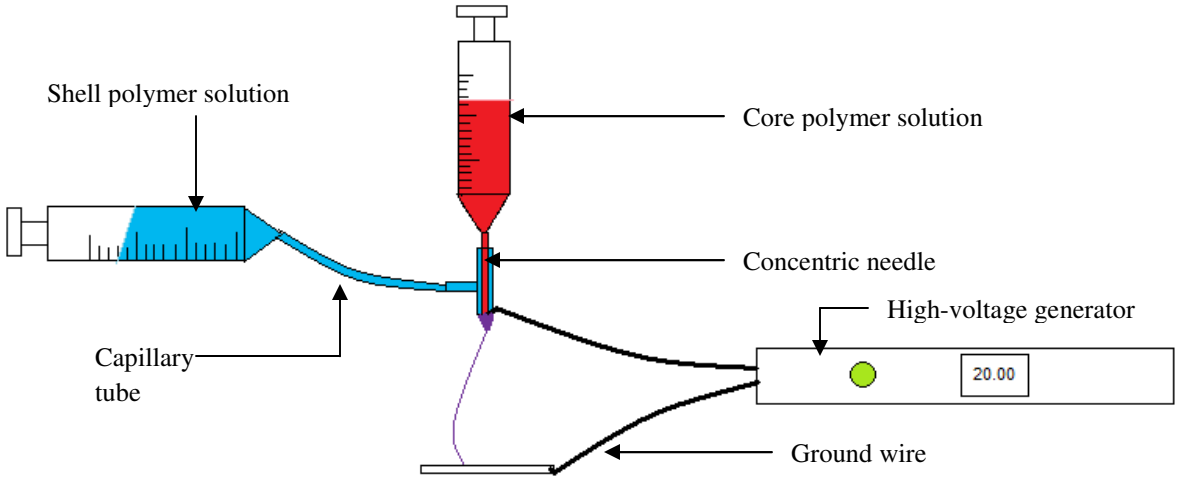

Figure 1: Coaxial spinning setup

2.2.3 Tensile Testing

Dogbones were cut out of the nanofiber samples and clamped in the load frame (SM-50-294, TestResources). The load frame was programmed to pull the ends of the dogbone apart and measure the force required to strain the samples. The program ran until the sample failed. This data was imported into an excel sheet and analyzed to determine the Young's Modulus of the samples. For each core-shell volume ratio, 5 samples were strained to failure to provide statistical validity.

2.2.4 Solubility Testing

To test the solubility of different polymers, the electrospun samples were first weighed. The samples were then exposed to vacuum for 24 hours to remove any residual HFP (Lannutti, J, OSU). PCL was exposed to vacuum at room temperature; PES at 60 °C. The samples were then re-weighed before being placed in a glass cover containing the solvent. Each sample used was approximately 1" by 1" in size. Each sample was exposed to 15 mL of solvent for 15 minutes. After exposure, the samples were retrieved and exposed to vacuum for 24 hours to remove any residual solvent from the fibers. The samples were then weighed and examined under the SEM.

3. Results and Discussion

3.1 Tensile Test Results

Tensile testing core-shell fibers of different core and shell flow rates provided the Young's Modulus of these fibers. The Young's Modulus was calculated by taking the slope of engineering stress vs. engineering strain graphs. This data is summarized in Figures 2 and 3 below. Tables 1 and 2 give the individual statistics of each graph. Figure 2 gives an overall picture of the relationship between core-shell flow rates and the fiber modulus. Figure 3 examines this relationship at a more detailed level involving gradual increments of different core-shell flow rates. Both graphs show that as the flow rate of the shell (PCL) increases relative to that of the core (PES), the Young's Modulus of the fiber also increases up to a point before it starts decreasing again. Both graphs illustrate that once the shell flow rate is more than double the core flow rate, stiffness begins decreasing. This indicates that as the PCL content increases relative to the PES content, the stiffness of the overall fiber matrix also increases. But once the PCL content of the overall core-shell fibers is greater than two times the PES content the stiffness decreases.

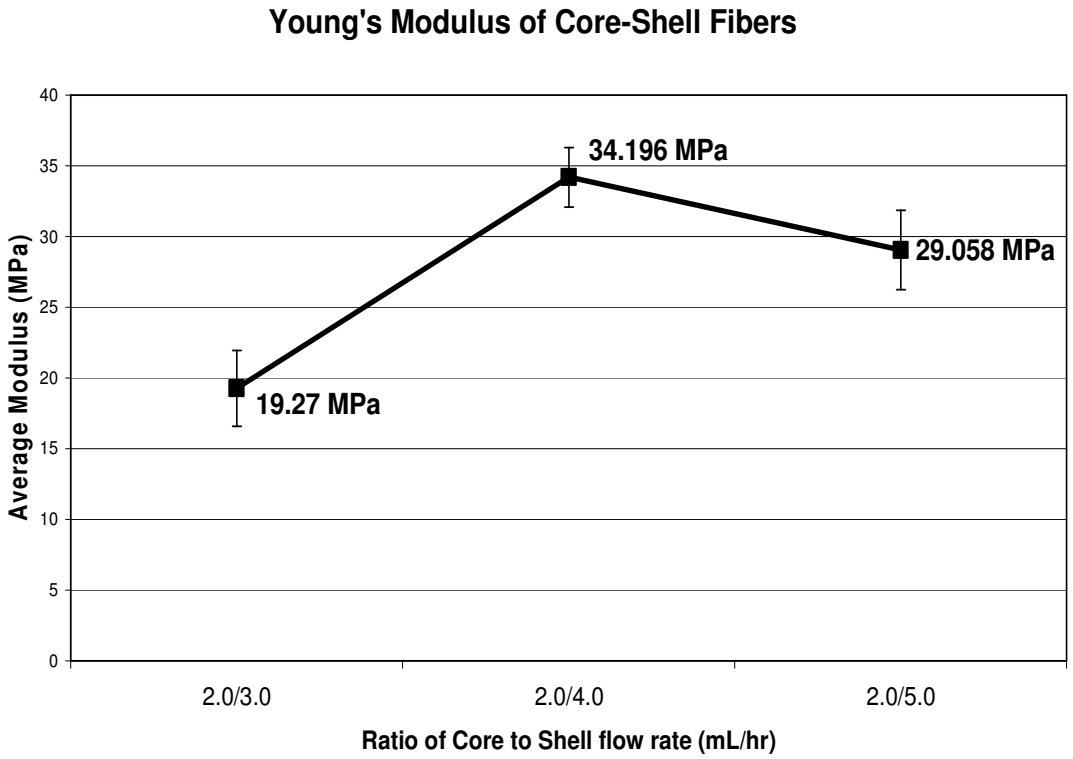

Figure 2: Average Young's modulus of core-shell fibers of different flow rates (Trial 1)

Table 1: Statistics for data graphed in Figure 2

Core-shell flow rates	Ave. UTS (MPa)	St. Dev of UTS	%Elongation	St. Dev of Elongation	Ave. Modulus (MPa)	St. Dev of Modulus
2.0/3.0	1.4342	0.1278	50.87536	3.38057	19.27	2.68141
2.0/4.0	2.9626	0.1852	88.78071	7.76113	34.196	2.11113
2.0/5.0	2.023	0.2563	41.71098	4.69186	29.058	2.81093

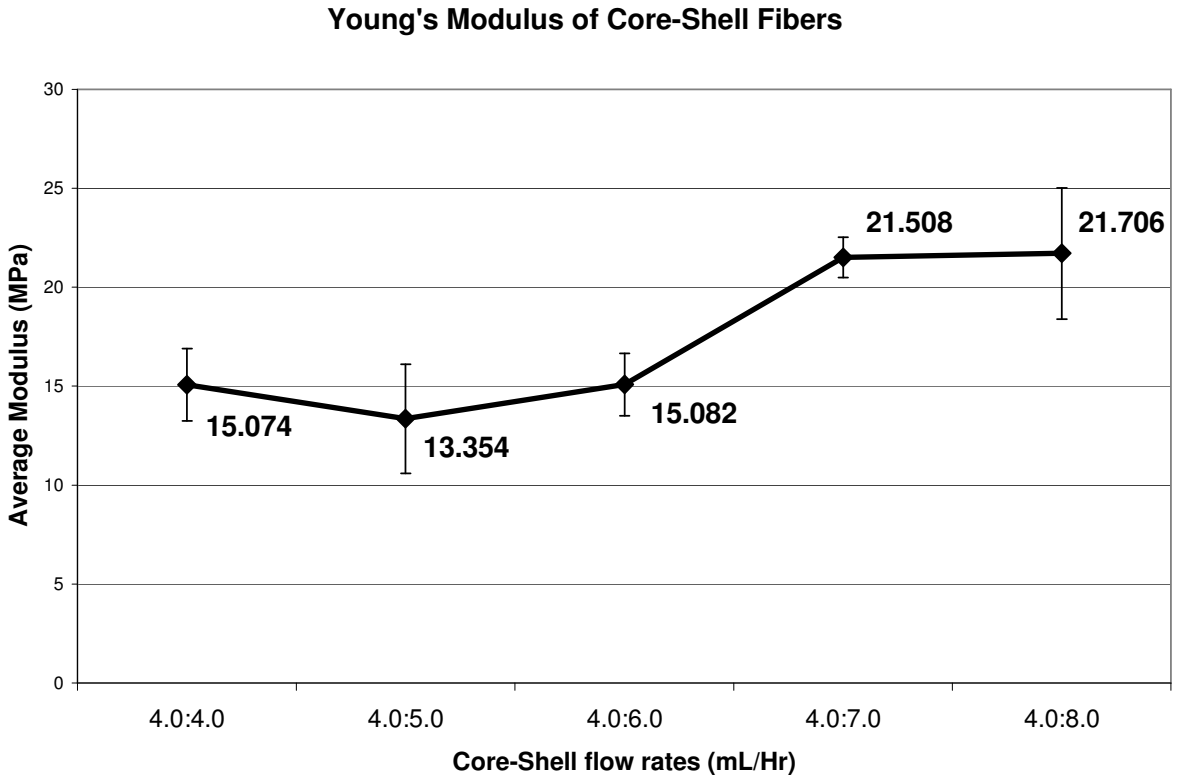

Figure 3: Average Young's modulus of core-shell fibers of different flow rates (Trial 2)

Table 2: Statistics for data graphed in Figure 3

Core-Shell flow rates (mL/Hr)	UTS (MPa)	St. Dev of UTS	% Elongation	St. Dev of %Elongation	Modulus of fibers (MPa)	St. Dev of Modulus
4.0:4.0	2.834	0.2568	119.187	6.813	15.074	3.638
4.0:5.0	2.541	0.952	92.528	12.888	13.354	5.512
4.0:6.0	2.467	0.516	111.273	32.285	15.082	3.157
4.0:7.0	3.033	0.2664	103.777	13.848	21.508	2.053
4.0:8.0	2.84	0.6535	87.53	20.244	21.706	6.609

3.2 Solubility Test Results

The various nanofiber samples were first subjected to qualitative testing with different solvents. These results are displayed in Table 3 below. These four particular solvents were chosen because of their lower polarity compared to HFP. In the table below, 'high dissolution'

refers to complete disappearance of the sample within a few seconds of immersion. 'Moderate dissolution' refers to the sample disappearance after a few minutes. 'Low dissolution' refers to sample presence in solid form after 15 minutes.

Table 3: Qualitative testing results with different solvents

Solvent	**Pure PCL**	**Pure PES**
Chloroform	High dissolution, no fiber remaining	High dissolution; no fiber but bubbles
Dichloromethane (DCM)	High dissolution, no fiber remaining	High dissolution, no fiber remaining
Tetrahydrofuran (THF)	High dissolution, no fiber remaining	Moderate dissolution; solidification of sheet
Trichloroethylene (TCE)	High dissolution, no fiber remaining	Low dissolution, fiber intact
Hexanes	Low dissolution, fiber intact	Low dissolution, fiber intact

From these qualitative observations, THF and TCE were isolated as potential solvents that could dissolve PCL over PES. Accordingly, quantitative solubility tests were conducted on several THF azeotropes with varying THF and water compositions. In these tests, the water used was distilled. The procedure outlined in the Methods section was followed except the PES and PCL samples were exposed to vacuum for 30 minutes only instead of 24 hours. The results are displayed below in Table 4 and Figure 4.

Table 4: PCL and PES solubility in THF azeotropes

Solvent azeotrope	% weight loss after exposure	
	PCL	PES
50% THF-50% H_2O	1.31%	8.02%
33% THF-67% H_2O	0.47%	11.08%
20% THF-80% H_2O	0.24%	10.86%
10% THF-90% H_2O	0.26%	10.71%

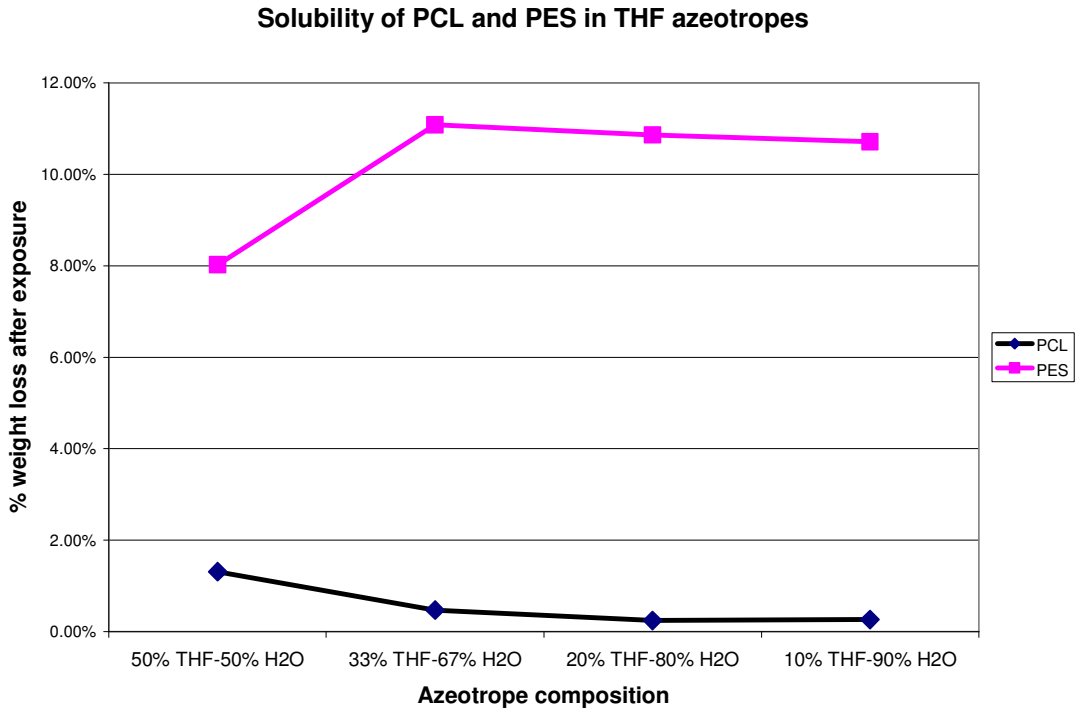

Figure 4: Solubility of pure PCL and PES in THF azeotropes

However, when the solubility test was re-conducted on the 33% THF azeotropes following the procedure outlined in the Methods section with a 24 hr vacuum period before exposure to solvent, the results were very different. The loss of PES mass was not as significant as previously observed, the total % weight loss being only 0.17%. This led to the conclusion that PES fibers could have been losing mass in the form of retained solvent trapped inside the polymer, not actual PES itself. This information led to the pursuit of hexanes as solvents. Solubility tests conducted on hexane as the solvent in the manner described in the Methods section yielded the results displayed in Table 5 below.

Table 5: Solubility of PCL and PES in straight chain hexanes

Fiber	Initial Mass	Final Mass	% weight loss
PCL	0.04476 g	0.04323 g	3.4182%
PES	0.02203 g	0.02163 g	1.8157%

Since the difference between PCL and PES in % dissolution in hexanes was not significant, TCE was examined as a potential solvent that could be used to preferentially dissolve PCL. The data collected from solubility tests on TCE are displayed in Table 6, 7, and 8 below.

Table 6: Solubility of PES in 100% TCE

PES Sample #	Initial Mass	Final Mass	% weight loss	Average	St. Dev
1	0.02297 g	0.02176 g	5.2677%	5.6681%	0.4547%
2	0.02115 g	0.01997 g	5.5792%		
3	0.02425 g	0.02284 g	6.4742%		
4	0.03587 g	0.03365 g	6.1890%		
5	0.02805 g	0.02651 g	5.4902%		

Table 7: Solubility of PCL in 100% TCE

PCL Sample #	Initial Mass	Final Mass	% weight loss	Average	St. Dev
1	0.04434 g	0 g	100	100%	0%
2	0.05654 g	0 g	100		
3	0.06375 g	0 g	100		
4	0.04932 g	0 g	100		
5	0.05219 g	0 g	100		

Table 8: Summary of solubility data in 100% TCE

Solvent	PCL % weight loss (Mean)	PES % weight loss (Mean)
TCE	100%	5.6681%

As can be seen from the data above, TCE showed exquisite selectivity toward PCL. PCL dissolved readily in TCE while PES showed very minimal dissolution. However, PES dissolution was not so small as to be considered negligible. To minimize % weight loss of PES in TCE, PES was tested in TCE-water and TCE-hexane mixtures. The data from these experiments are given in Tables 9 and 10.

Table 9: Solubility of PES in 10% water - 90% TCE mixtures

PES Sample #	Initial Mass	Final Mass	% Weight Loss	Average	St. Dev
1	0.01534 g	0.01390 g	9.3872%	8.9334%	0.3884%
2	0.01742 g	0.01595 g	8.4386%		
3	0.00858 g	0.00781 g	8.9744%		

Table 10: Solubility of PES in 10% Hexane - 90% TCE mixtures

PES Sample #	Initial Mass	Final Mass	% weight loss	Average	St. Dev
1	0.01350 g	0.01291 g	4.3704%	4.5802%	0.2252%
2	0.01139 g	0.01088 g	4.4776%		
3	0.01165 g	0.01108 g	4.8927%		

As can be observed data presented above, the solubility of PES seemed to decrease as the hexane portion in the TCE mixture increased. To examine this trend further, solubility of PES was tested in a few more TCE-Hexane mixtures. The data is given in Tables 11 and 12 below. % weight loss of PCL in all the mixtures tested below was 100% with a standard deviation of 0. All the data presented so far on TCE as a solvent are graphically presented in Figure 5 below.

Table 11: Solubility of PES in 20% Hexane - 80% TCE mixtures

PES Sample #	Initial Mass	Final Mass	% weight loss	Average	St. Dev
1	0.01186 g	0.01140 g	3.8786%	3.6840%	0.6136%
2	0.01016 g	0.00987 g	2.8543%		
3	0.00903 g	0.00864 g	4.3189%		

Table 12: Solubility of PES in 33% Hexane – 67% TCE mixtures

PES Sample #	Initial Mass	Final Mass	% weight loss	Average	St. Dev
1	0.00822 g	0.00789 g	4.0146%	3.1573%	0.6757%
2	0.00804 g	0.00785 g	2.3632%		
3	0.00808 g	0.00783 g	3.0941%		

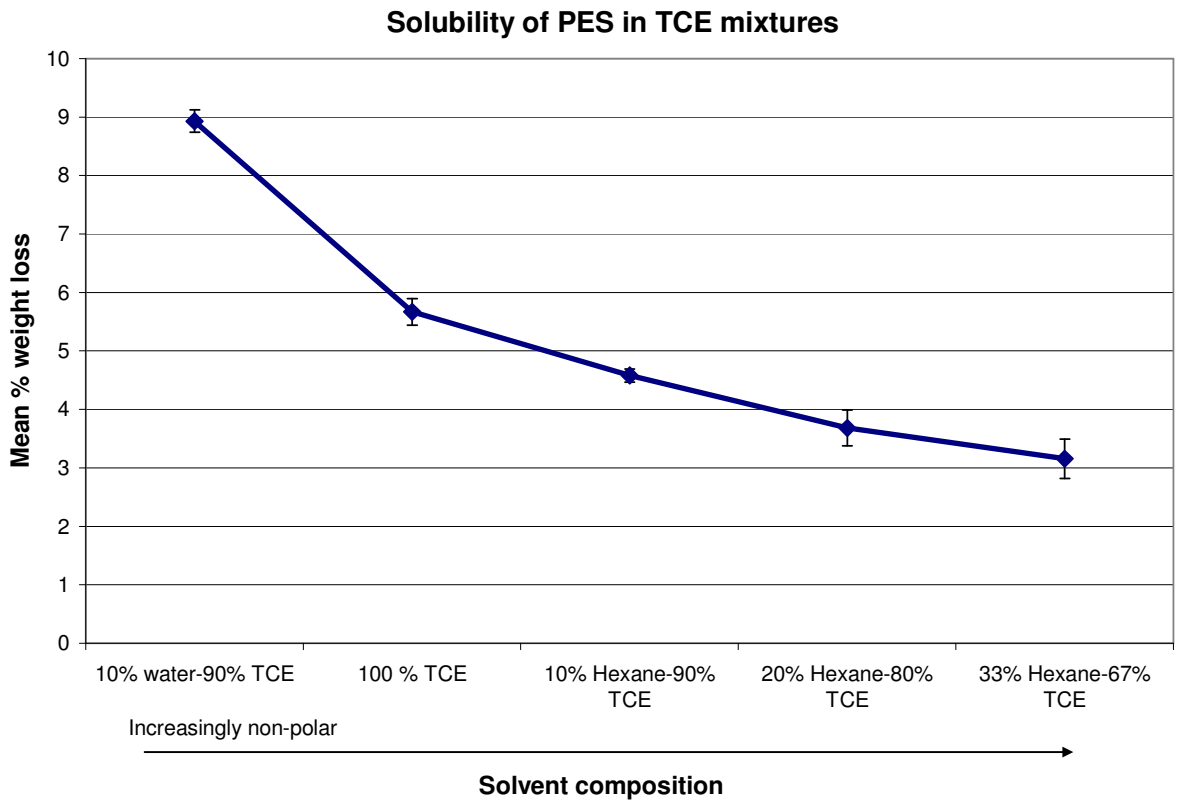

Figure 5: Solubility trends observed in TCE mixtures

As can be seen from the graph above, the solubility of PES increased as the TCE solvent mixture became increasingly non-polar. However, the decrease in solubility was not close to zero in any of the solvent mixtures. This led to a tentative prediction that PES nanofiber samples may contain low molecular weight species that dissolve and separate from the matrix regardless of the solvent. To test this hypothesis, the PES samples that were exposed to TCE were cycled through TCE again after a second exposure to 24 hours of vacuum. The results from this experiment are presented in Table 13 below.

Table 13: Results from exposing PES to 100% TCE a second time

PES Sample #	Initial Mass	Mass After Cycle 1	% weight change after cycle 1	Mass After Cycle 2	% weight change after cycle 2
1	0.00849 g	0.00790 g	-6.9494%	0.00789 g	0.1266%
2	0.00466 g	0.00429 g	-7.9399%	0.00432 g	-0.6993%
3	0.00467 g	0.00438 g	-6.2099%	0.00430 g	1.8265%
4	0.00627 g	0.00582 g	-7.1770%	0.00582 g	0
5	0.01306 g	0.01240 g	-5.0536%	0.01244 g	-0.3226%
Average	N/A	N/A	-6.6659	N/A	0.1862
St. dev	N/A	N/A	0.9770	N/A	0.8685

It can be observed from Table 13 above that the % weight loss of PES was close to zero after the PES samples were cycled through TCE a second time. This confirms the hypothesis that PES contains small amount of low molecular weight species that dissolve regardless of the solvent used.

From the data presented so far, it can be concluded that TCE is the best solvent for preferential dissolution of PCL over PES. Having reached this conclusion, core-shell fibers were exposed to TCE and their weight loss recorded. The results from this experiment are presented in Table 14 below.

Table 14: Solubility of PES-PCL core-shell fibers in TCE

Core-shell flow rates (mL/hr)	PCL Content	Initial Mass	Final Mass	% Weight loss
2:2	50%	0.00951 g	0.00794 g	16.51%
2:3	60%	0.01147 g	0.00900 g	21.53%
2:4	67%	0.00925 g	0.00655 g	29.19%

The core-shell fibers lost more weight as the PCL content of the core-shell fibers was increased. As can be seen in Figure 6 below, the increase in % weight loss does corresponds almost linearly with the increase in % PCL content.

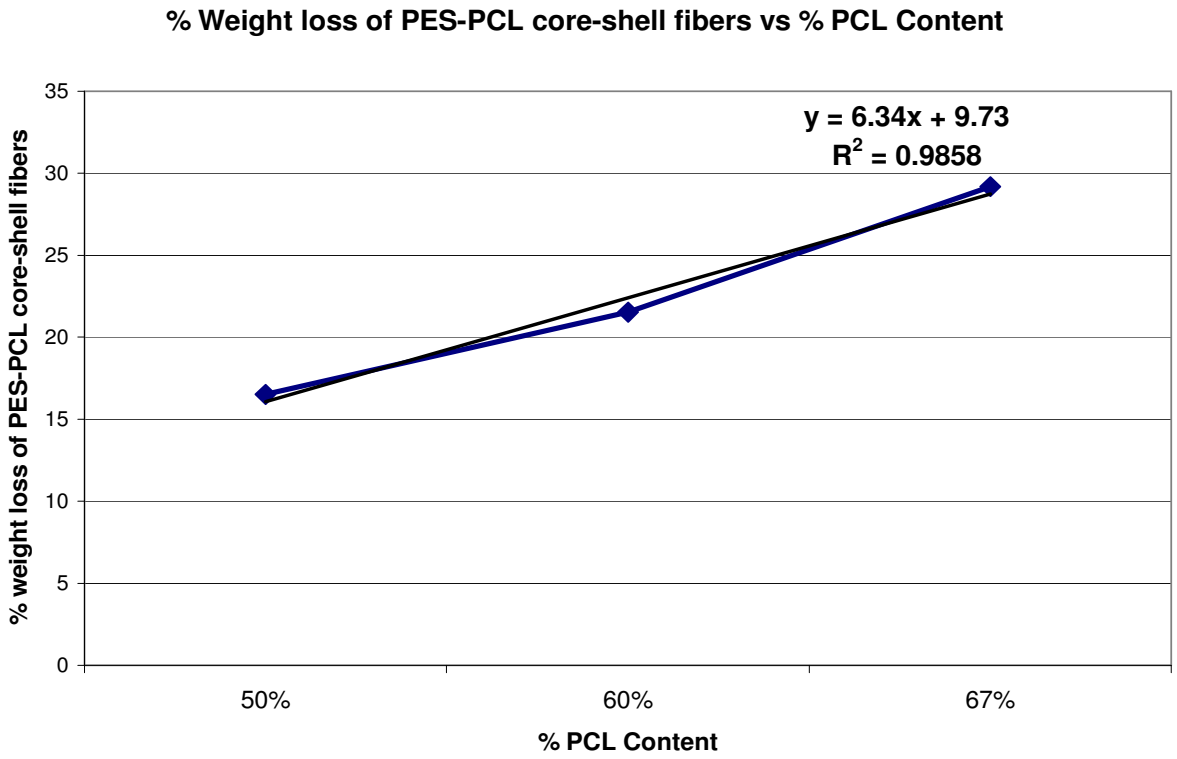

Figure 6: Percentage weight loss of core-shell fibers with increasing PCL content

Though a positive, linear relationship was observed between PCL content and overall weight loss observed in core-shell fibers after exposure to TCE, the % weight loss was not equal to % PCL content. This is unexpected, considering the fact that pure PCL was shown to dissolve 100% in TCE. Furthermore, webbing was observed in SEM images, as can be seen in Figures 7, 8, and 9.

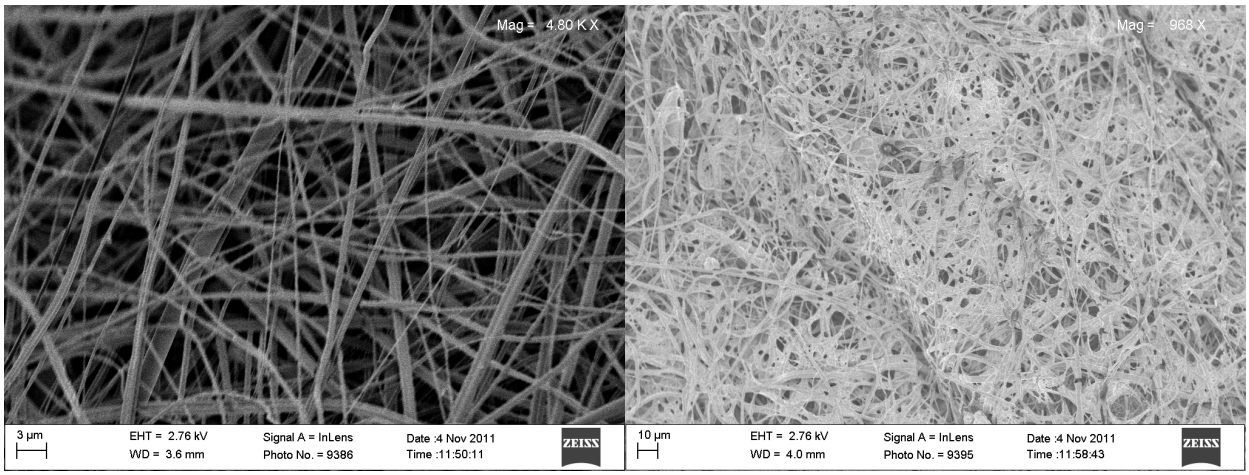

Figure 7: (Left) 2:2 original core-shell fibers; (Right) 2:2 core-shell fibers after TCE exposure

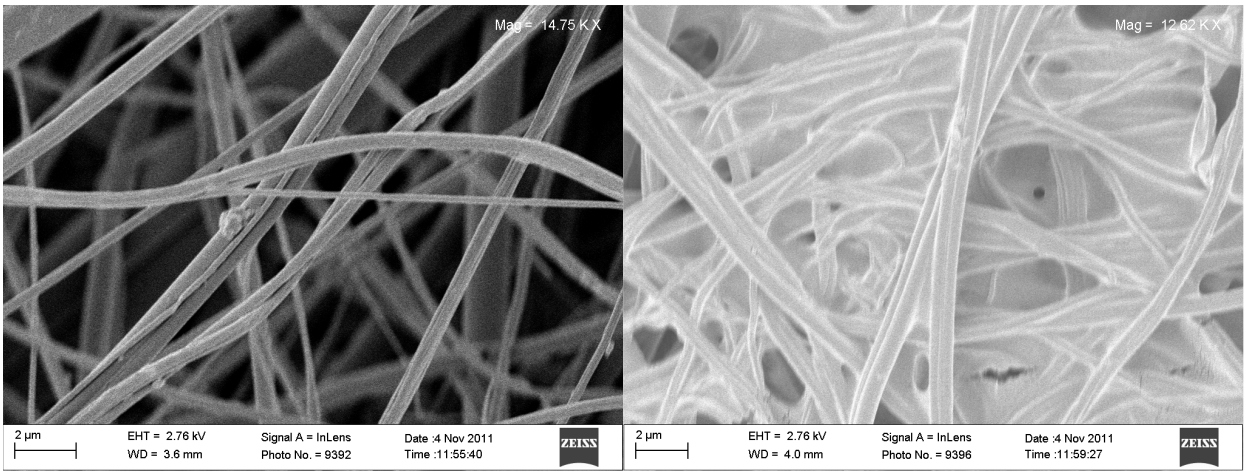

Figure 8: (Left) 2:2 original core-shell fibers; (Right) 2:2 core-shell fibers after TCE exposure

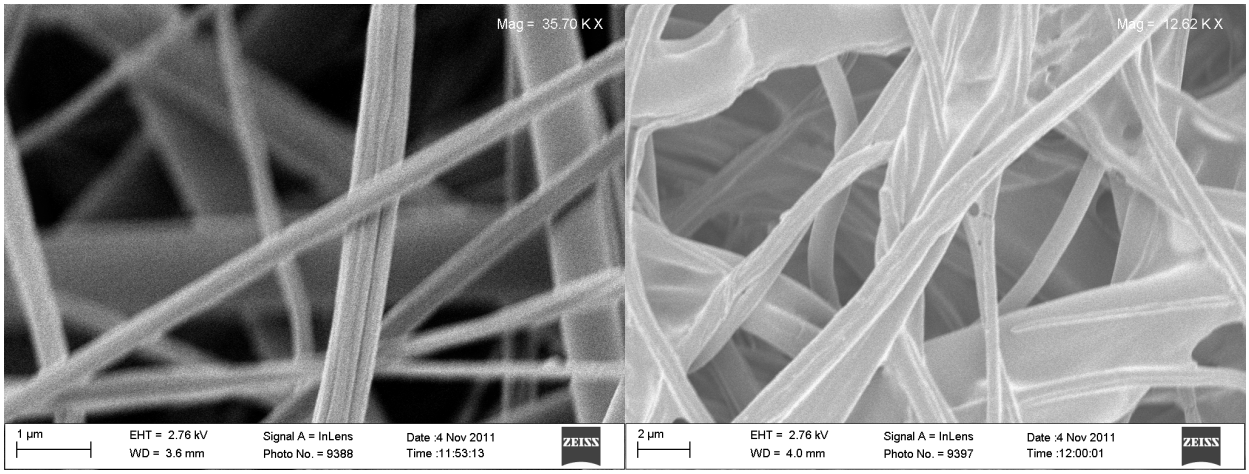

Figure 9: (Left) 2:2 original core-shell fibers; (Right) 2:2 core-shell fibers after TCE exposure

This led to the hypothesis that the supposedly separate PES and PCL may be chemically intermingling with each other when they are electrospun as core-shell fibers and this interaction prevents complete dissolution of the PCL shell from core-shell fibers. To investigate this theory, several PES/PCL blends were tested for their solubility in TCE. All the blends were 6.7 wt% solutions with HFP as the solvent. A brief qualitative analysis yielded the observations tabulated in Table 15 below.

Table 15: Solubility of PES/PCL blends in TCE – visual observations

Blend (6.7 wt% solutions)	Observations
5% PES – 95% PCL	High dissolution, no fiber remaining
10% PES – 90% PCL	High-moderate dissolution, no fiber remaining
20% PES – 80% PCL	Moderate dissolution, thin film observed

The 5% and 10% PES blends resulted in dissolution of the fiber to such as extent that the fiber was no longer in solid form. SEM images of these two blends are given in Figure 10. Fiber-fiber bonding can be observed in both the images below. This microstructure could explain why stiffness of the core-shell fibers increased as the PCL content increased. As the PCL content increased, fiber-fiber bonding also increased; this resulted in a higher stiffness.

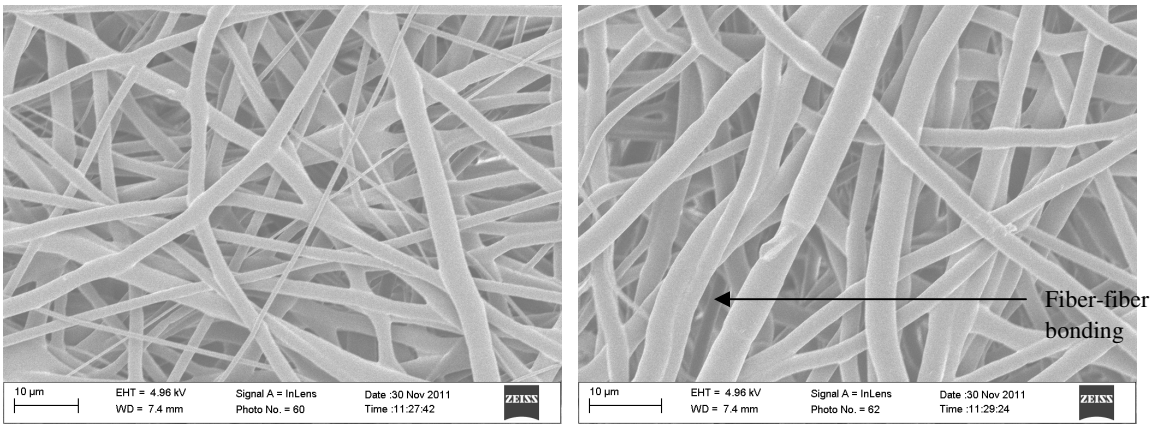

Figure 10: (Left) Orig. 5% PES - 95%PCL blend; (Right) Orig. 10% PES – 90% PCL blend

The 20% blend fiber was still intact as a thin film after exposure to TCE. Hence, quantitative analysis was done on the 20% fiber blend. The results are presented in Table 16.

Table 16: Solubility of 20% PES/80% PCL fiber blend in TCE

20% Blend Sample #	Initial Mass	Final Mass	% Weight Loss	Average	St. Dev
1	0.01094 g	0.00771 g	29.525%	36.8049%	5.1529%
2	0.00850 g	0.00508 g	40.235%		
3	0.00725 g	0.00494 g	31.862%		
4	0.00477 g	0.00273 g	42.767%		
5	0.00603 g	0.00364 g	39.635%		

The above data suggest that PES-PCL interaction is indeed going on because with an introduction of even a small percent of PES, the % weight loss of PCL when exposed to TCE decreases substantially. The hypothesis that this interaction may be the cause of the 'webbing' observed in core-shell fibers after TCE exposure is supported by the SEM image of the PES/PCL blend given below in Figure 11.

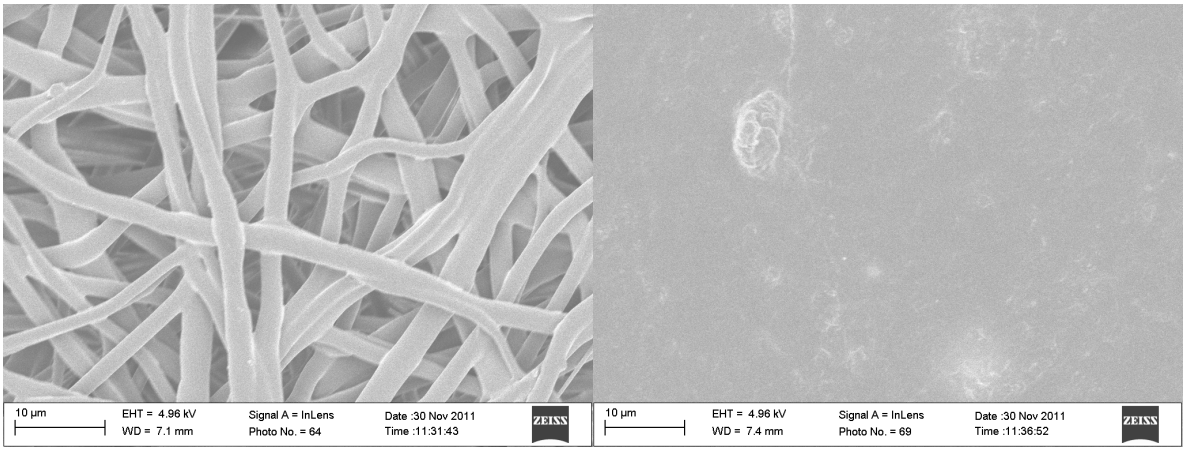

Figure 11: (Left) Original 20% PES-80% PCL blend; (Right) Same blend after TCE exposure

The lack of fibers in the image above gives proof to the theory that PES-PCL interactions in the core-shell fibers are preventing the complete dissolution of the shell.

4. Conclusions

4.1 Summary

The overall goals of this project were the following: (1) determine the mechanical properties of PES-PCL core-shell properties; (2) identify a solvent that dissolves PCL but not PES.

The mechanical behavior of PES-PCL core-shell fibers was studied by examining the relationship between the fiber stiffness and fiber composition. This experiment revealed that as the PCL content in the core-shell fibers is increased, the overall stiffness of the fiber also increases. But this trend only applies until the PCL content is approximately double the PES content. After this point, the stiffness decreases again as the PCL content is increased.

After studying several potential solvents, it was determined that TCE is the best solvent for preferentially dissolving PCL (100% dissolution) and not PES (virtually zero dissolution). However, PCL and PES interact with each other when they are in core-shell form and this interaction prevents the complete dissolution of PCL shell in the core-shell fibers upon exposure to TCE. This results in webbing and fiber disintegration. This hypothesis is supported by SEM analysis of PES/PCL blends.

4.2 Future Work

The data produced in this project proves that core-shell fibers spun under these conditions are in fact a trilayer structure that includes a layer consisting of a blend of PES and PCL. This information could help determine how much of the mechanical behavior of the core-shell fibers is due to the structure and arrangement of fibers and how much of it is due to the compositional arrangements within the fibers.

Furthermore, further studies can be done on the core-shell fiber mechanical properties by examining the effect of fiber diameter on the stiffness and UTS of the fiber. This information could again help investigate the effect of physical structure of the fibers on the mechanical properties versus the effect of the chemical composition of the fibers on the mechanical behavior.

References

[1] Gurski LA, Petrelli NJ, Jia X, et al. 3D Matrices for Anti-Cancer Drug Testing and Development. *Oncology Issues* 2010; 25: 20-25.

[2]Gurski LA, Jha AK, Zhang C, et al. Hyaluronic acid-based hydrogels as 3D matrices for in vitro evaluation of chemotherapeutic drugs using poorly adherent prostate cancer cells. *Biomaterials* 2009; 30:6076- 6085.

[3]Feder-Mengus C, Ghosh S, Reschner A, et al. New dimensions in tumor immunology: what does 3D culture reveal? *Trends Mol Med.* 2008; 14:333- 340.

[4]Santini MT, Rainaldi G, Romano R, et al. MG-63 human osteosarcoma cells grown in monolayer and as three-dimensional tumor spheroids present a different metabolic profile: a (1)H NMR study. *FEBS Lett.* 2004; 557:148-154

[5]David L, Dulong V, Le Cerf D, et al. Hyaluronan hydrogel: an appropriate three-dimensional model for evaluation of anticancer drug sensitivity. *Acta Biomater.* 2008; 4:256-263.

[6]Horning JL, Sahoo SK, Vijayaraghavalu S, et al. 3-D tumor model for in vitro evaluation of anticancer drugs. *Mol Pharm.* 2008; 5:849-862.

[7] Sun T, Jackson S, Haycock JW, et al. Culture of skin cells in 3D rather than 2D improves their ability to survive exposure to cytotoxic agents. *Journal of Biotechnology* 2005; 122(3): 372-381.

[8] Mo XM, Xu CY, Kotaki M, et al. Electrospun P(LLA-CL) nanofiber: a biomimetic extracellular matrix for smooth muscle cell and endothelial cell proliferation. *Biomaterials* 2004; 25(10): 1883-1890.

[9] Tibbitt MW, Anseth KS. Hydrogels as extracellular matrix mimics for 3D cell culture. *Biotechnology and Bioengineering* 2009; 103(4): 655-663.

[10] Salinas CN, Anseth KS. 2008a. Mixed mode thiol-acrylate photopolymerizations for the synthesis of PEG-peptide hydrogels. *Macromolecules* 41(16):6019–6026.

[11] Zhang YZ, Su B, Venugopal J, et al. Biomimetic and bioactive nanofibrous scaffolds from electrospun composite nanofibers. *Int J Nanomedicine* 2007; 2(4): 623-638.